Magnetic field measurements in laser-produced plasmas via proton deflectometry

Cecchetti, C. A., Borghesi, M., Fuchs, J., Schurtz, G., Kar, S., Macchi, A., ... Neely, D. (2009). Magnetic field measurements in laser-produced plasmas via proton deflectometry. Physics of Plasmas, 16(4), 043102-043102-5. [043102]. DOI: 10.1063/1.3097899

Published in:
Physics of Plasmas

Document Version:
Publisher's PDF, also known as Version of record

Queen's University Belfast - Research Portal:
Link to publication record in Queen's University Belfast Research Portal

Magnetic field measurements in laser-produced plasmas via proton deflectometry

C. A. Cecchetti, M. Borghesi, J. Fuchs, G. Schurtz, S. Kar et al.

Citation: Phys. Plasmas **16**, 043102 (2009); doi: 10.1063/1.3097899
View online: http://dx.doi.org/10.1063/1.3097899
View Table of Contents: http://pop.aip.org/resource/1/PHPAEN/v16/i4
Published by the American Institute of Physics.

Magnetic field measurements in laser-produced plasmas via proton deflectometry

C. A. Cecchetti,[1,a)] M. Borghesi,[1] J. Fuchs,[2] G. Schurtz,[3] S. Kar,[1] A. Macchi,[1,b)] L. Romagnani,[1] P. A. Wilson,[1] P. Antici,[2,c)] R. Jung,[4] J. Osterholtz,[4] C. A. Pipahl,[4] O. Willi,[4] A. Schiavi,[5] M. Notley,[6] and D. Neely[6]

[1]*School of Mathematics and Physics, Queen's University of Belfast, Belfast BT7 1NN, United Kingdom*
[2]*LULI, École Polytechnique, CNRS/CEA/UPMC, Route de Saclay, 91128 Palaiseau, France*
[3]*Centre d'Etudies des Lasers Intenses et Applications, Universitè Bordeaux I, UMR 5107, CNRS, CEA, 33405 Talence, France*
[4]*Institut für Laser und Plasma Physik, Heinrich-Heine-Universität Düsseldorf, 40225 Dusseldorf, Germany*
[5]*Dipartimento di Energetica, Università di Roma 1 "La Sapienza," via Scarpa 14-16, 00161 Roma, Italy*
[6]*Central Laser Facility, Science and Technology Facilities Council, Rutherford Appleton Laboratory, Harwell Science and Innovation Campus, Didcot OX11 0QX, United Kingdom*

(Received 13 August 2008; accepted 10 February 2009; published online 3 April 2009)

Large magnetic fields generated during laser-matter interaction at irradiances of $\sim 5 \times 10^{14}$ W cm^{-2} have been measured using a deflectometry technique employing MeV laser-accelerated protons. Azimuthal magnetic fields were identified unambiguously via a characteristic proton deflection pattern and found to have an amplitude of ~45 T in the outer coronal region. Comparison with magnetohydrodynamic simulations confirms that in this regime the $\vec{\nabla} T_e \times \vec{\nabla} n_e$ source is the main field generation mechanism, while additional terms are negligible.
 [DOI: 10.1063/1.3097899]

I. INTRODUCTION

The characterization of self-generated magnetic fields is an important issue in laser-plasma experiments. It is of particular relevance in the context of inertial confinement fusion (ICF) where magnetic fields strongly affect energy transport (Refs. 1–3 and references therein). In this context, detailed measurements of magnetic fields with spatial and temporal resolution are needed to validate computational codes or models.[3–6] The measurement of laser-produced magnetic fields in conditions relevant to "conventional" ICF (i.e., with laser intensities up to $\sim 10^{15}$ W cm^{-2}) has been limited so far to the outer "coronal" plasma region (with densities up to 10^{20} cm^{-3}), where magnetic fields of amplitude up to the order of 10^2 T generated due to the $\vec{\nabla} T_e \times \vec{\nabla} n_e$ mechanism[1] have been identified via optical polarimetry.[1,7,8] Denser plasma regions could not be optically probed because of their high index of refraction.

In this article we report on the measurements of magnetic fields using a deflectometry technique employing laser-accelerated protons,[9,10] capable of accessing a wide range of densities, from solid density down to the tenuous coronal plasma. The magnetic fields were self-generated as a result of the interaction between a nanosecond pulse of intensity of $\sim 5 \times 10^{14}$ W cm^{-2} and a thin aluminum foil. Using protons with energy up to 15 MeV, we characterized magnetic fields of amplitude up to ~45 T. The present technique may in principle be extended to the detection of larger magnetic fields (>100 T) by using probe protons with higher energy. Although proton probing techniques have mainly been applied to the study of transient electric fields in intense laser-matter interaction,[10,11] particular deflection patterns observed in some experiments have highlighted the presence of large magnetic fields.[12] Recent investigations on magnetic fields in laser-produced plasmas were recently reported by Nilson *et al.*[13] using a similar deflectometry technique with laser-accelerated protons and by Li *et al.*[14] employing protons generated from laser-driven implosions requiring a kilojoule laser driver. In ultrahigh intensity interactions, very large fields ($\geq 10^4$ T) have been revealed via polarization changes induced on high harmonics;[15] such technique, however, does not allow spatially and temporally resolved field mapping and is not applicable to moderate intensity, ICF-relevant interactions. In general, proton deflection measurements from a single probing direction cannot distinguish unambiguously between the effects of electric and magnetic fields. In this article it is shown that the protons are deflected by azimuthal magnetic fields (having rotational symmetry with respect to the probe axis) through an inversion of the proton deflection pattern when the proton probing direction is reversed, i.e., the sign of the proton velocities is changed in the magnetic component of the Lorentz force $e\vec{v} \times \vec{B}$. Simultaneous transverse and axial probing on the same plasma are also carried out to verify further the dominance of magnetic fields with respect to electric fields in producing the deflectometry patterns. Our experimental measurements are supported by the numerical reconstruction of proton deflectometry images using a particle tracing code calculating the probe proton deflections in assigned electromagnetic fields and by magneto-

[a)]Present address: IPCF, CNR, Area Della Ricerca di Pisa, via G. Moruzzi 1, 56124 Pisa, Italy.
[b)]On leave from polyLAB, CNR/INFM, Pisa, Italy.
[c)]Also at Dipartimento di Energetica, Università di Roma 1 "La Sapienza," via Scarpa 14-16, 00161 Roma, Italy.

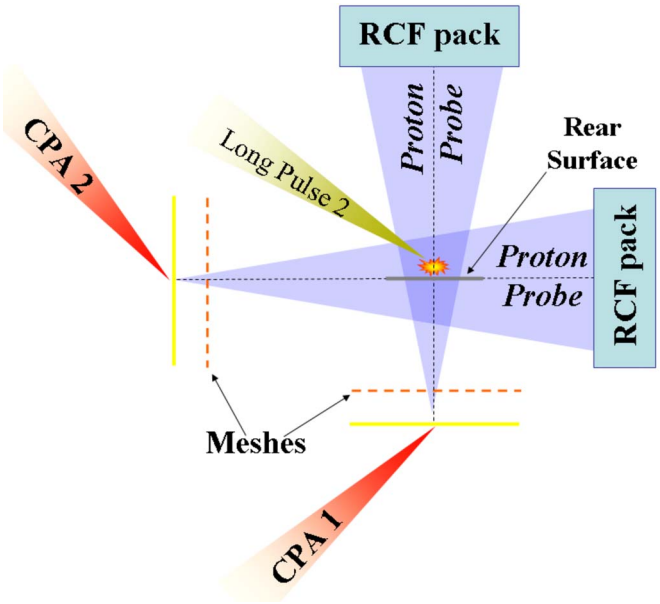

FIG. 1. (Color online) Schematic of the experimental setup. Only the rear-side interaction pulse is shown.

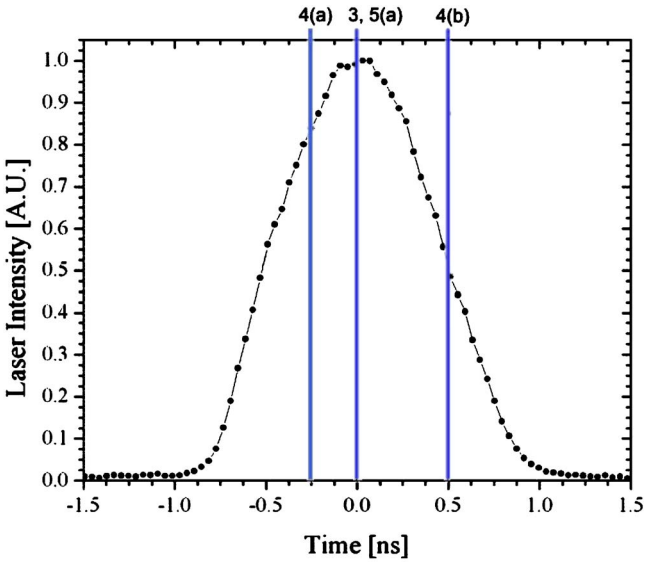

FIG. 2. (Color online) Temporal profile of the ns interaction pulse as obtained on a streak camera. The relative delays at which the deflectograms shown in this manuscript have been taken are overlaid on the profile, with reference to the figure numbers.

hydrodynamics (MHD) simulations using the CHIC code.[16] The comparison between experimental data and simulations shows that $\vec{\nabla}T_e \times \vec{\nabla}n_e$ is the dominant magnetic field source term and no detectable fields are produced in the inner, dense plasma zone.

II. EXPERIMENTAL ARRANGEMENT

The experiment was performed at the Rutherford Appleton Laboratory (RAL) using the Vulcan Nd:glass laser. In Fig. 1 the experimental setup is shown. Targets consisting of 6 μm thick Al foils were irradiated with 50 J, 1 ns duration laser pulses at a wavelength of 1 μm. Targets have been alternatively irradiated at the front and rear surface in separated shots with two different laser beams. These beams were focused with $f/10$ lenses to a focal spot radius of 50 μm at $\sim 60°$ with respect to the normal to the target plane resulting in on-target intensities in the range of $3-6\times10^{14}$ W cm^{-2}. Figure 1 shows one of the two irradiation arrangements. The polarization was linear, mixed between *S* and *P* due to the setup arrangement. Slowly varying electric and magnetic field structures produced in the laser-plasma interaction were investigated using point-projection proton probing in the deflectometry arrangement. Two proton probe beams (up to 15 MeV in energy) were accelerated[10,17] by irradiating two Au solid foils (25 μm thick) with 50 J, 1 ps laser pulses produced by chirped pulse amplification (CPA) focused to focal spots of 10 μm in radius, resulting in an on-target intensity of 5×10^{18} W cm^{-2}. The two proton beams were used to probe the plasma produced by the nanosecond pulse along two perpendicular probing directions, as schematically shown in Fig. 1. With this arrangement, in every shot two proton deflection maps were simultaneously obtained, one of which was face on, i.e., with the proton probe axis parallel to the plasma axis, and the other one was side on, i.e., with the proton probe axis parallel to the target surface. Depending on which nanosecond pulse was used, the plasma was probed by the face-on proton beam in two different configurations: interaction placed at the rear surface of the target (*rear interaction*) or interaction facing the incoming probing beam (*front interaction*), see Fig. 1. This allowed for the face-on beam to probe the plasma produced on either side of the target and thus to identify unambiguously the effect of azimuthal magnetic fields (having rotational symmetry with respect to the axis of the proton probe). A multilayer stack of radiochromic films was employed as the detector. A 1500 line/inch Cu mesh was inserted between the proton target and the probed plasma in the standard deflectometry arrangement.[9,10] The spatial resolution was a few tens of microns, as determined by the mesh spacing. The temporal resolution is determined by the transit time of protons across the probed field structure; for 5.5 MeV protons and a typical size of ~ 100 μm, one obtains ~ 3 ps. The delay between the two CPA pulses and the nanosecond pulse was varied throughout the experiment to investigate the temporal evolution of the electric and magnetic fields at various stages of the laser pulse irradiation, see Fig. 2.

III. EXPERIMENTAL RESULTS

Figure 3 shows the face-on deflectograms taken at the peak of the nanosecond pulses (~ 0 ps) in rear and front interaction configurations. By comparing Figs. 3(a) and 3(c), it is observed that, while in rear interactions the protons are deflected outward, causing the stretching of the mesh elements (consistently with previously published observations[14]), in the other case the mesh lines are compressed inward. This effect is a demonstration of the presence of a magnetic field, as inverting the probing direction would not affect the transverse deflection if this was mainly caused by radial electric fields in the plasma. Although a compression effect is clear and the difference with the *rear*

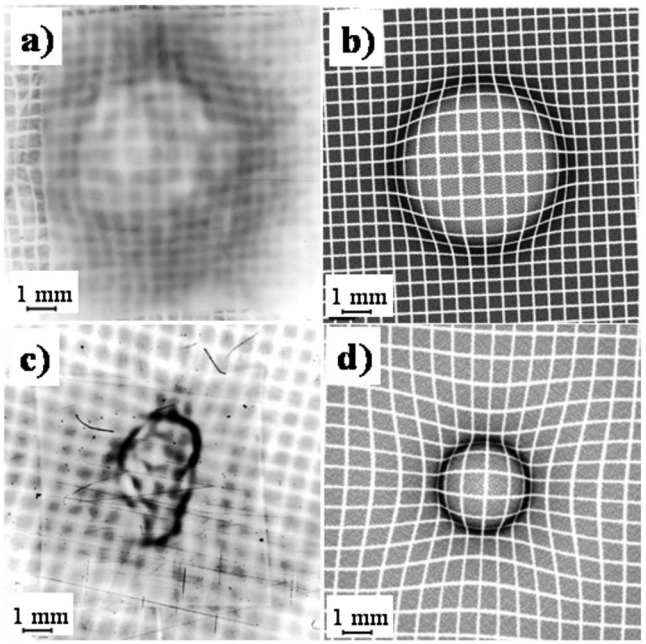

FIG. 3. (a) Typical face-on probing deflectogram in rear interaction configuration using 5.5 MeV protons, magnification $M=11$. (b) PTRACE simulations for the conditions of (a) assuming the toroidal $\vec{B}$ distribution parametrized as in Eq. (3). [(c) and (d)] Same interaction conditions as (a) and (b) but front interaction, $M=13$ and 7 MeV protons. The parameters of the PTRACE simulations [see Eq. (3)] are $B_0=-45$ T, $r_B=150$ μm, $L_r=150$ μm, $z_B=0$, $L_{z1}=200$ μm, are $L_{z2}=60$ μm. The polarity of $\vec{B}$ is inverted in (d). The timing of the data shown corresponds approximately to the pulse peak.

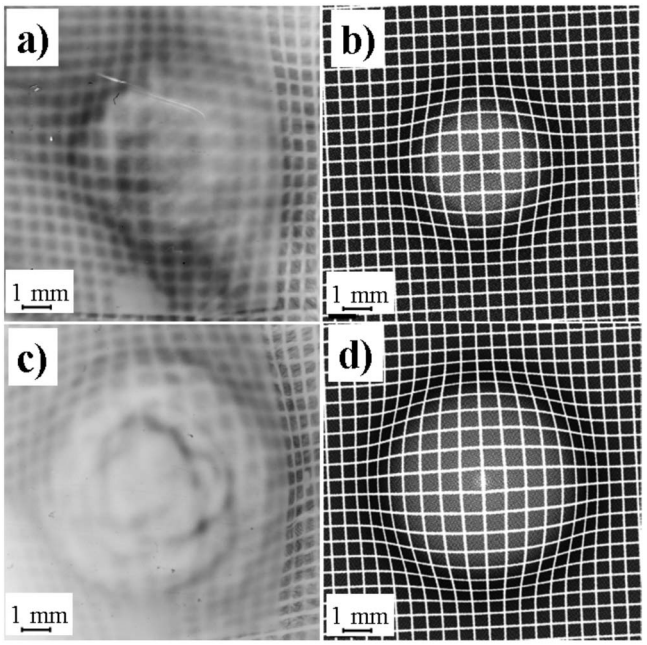

FIG. 4. (a) Face-on probing deflectograms in rear configuration taken at $t=-250$ ps using 5.5 MeV protons, geometrical magnification $M=13$. (b) The corresponding PTRACE simulation with parameters $B_0=-35$ T, $r_B=120$ μm, $L_r=150$ μm, $z_B=0$, $L_{z1}=150$ μm, and $L_{z2}=40$ μm. [(c) and (d)] Same as (a) and (b) but at $t=500$ ps; the simulation parameters in (d) are $B_0=-45$ T, $r_B=180$ μm, $L_r=200$ μm, $z_B=0$, $L_{z1}=200$ μm, and $L_{z2}=60$ μm.

configuration data is striking, the pattern in Fig. 3 presents some asymmetry likely due to a nonideal intensity distribution across the focal spot of the interaction beam used in the *front configuration*.

Figures 4(a) and 4(c) show the face-on images relative to different shots in which the proton beams probed the plasma respectively earlier (by ~250 ps) and later (by ~500 ps) as compared to Fig. 3. The distortion of the mesh pattern is mainly due to the magnetic field "lens effect" as already mentioned, and a clear evolution in terms of fringe deflection and pattern dimension is visible. Figure 5(a) shows a side-on deflectometry image taken simultaneously to the face-on image of Fig. 3(a). In such side-on data only a small deflection of the mesh pattern is observed. This is consistent with the face-on data suggesting a leading effect of an azimuthal magnetic field. A field distribution localized around a particular z position (e.g., resembling a magnetic torus) may indeed produce the small deflection observed in side-on images because a test proton, due to its displacement along z as it enters the field region, crosses two regions with fields of opposite directions but different amplitudes, whose effects partially compensate each other.

IV. MHD SIMULATIONS

The generation of an azimuthal magnetic field in the present experimental conditions is confirmed by simulations performed using CHIC,[16] a two-dimensional (2D) Lagrangian MHD code devoted to ICF related studies and developed at CELIA (Bordeaux). The code includes a two temperature plasma model, equations of state, and nonequilibrium radiation transport. Laser energy absorption is modeled via inverse Bremsstrahlung. The transverse MHD package of CHIC takes into account pressure-driven magnetic source terms, resistive diffusion of magnetic field, and Spitzer thermal conduction with magnetic inhibition. Starting from generalized Ohm's law and with suitable assumptions (i.e., neglecting radiation effects, both thermal and ponderomotive, and assuming an isotropical conductivity) the equation for the magnetic field is

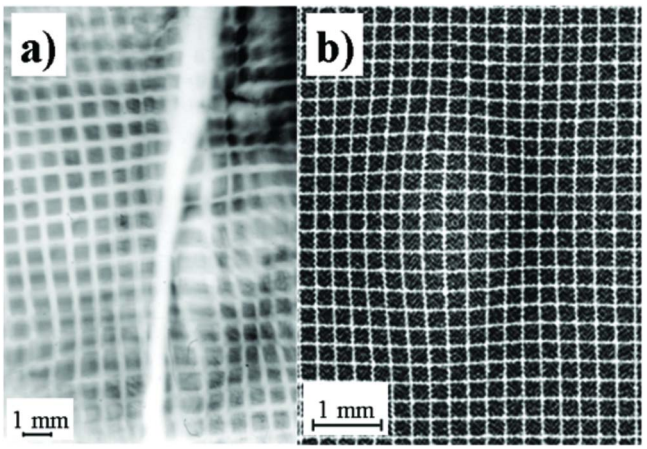

FIG. 5. (Color online) (a) Side-on probing deflectogram obtained simultaneously with the face-on image in Figs. 3(a) and 3(b): the corresponding PTRACE simulation.

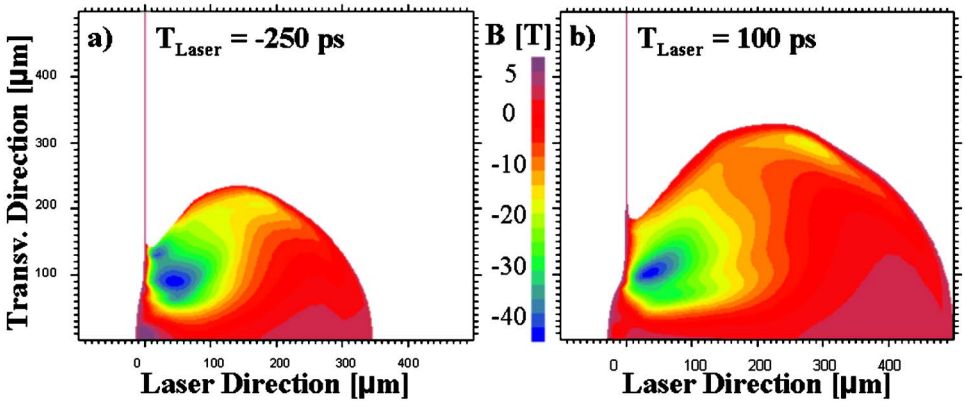

FIG. 6. (Color online) MHD simulation with the CHIC code. Parameters are laser intensity $I=5\times10^{14}$ W cm^{-2}, 50 μm spot radius, and $Z=13$ ion charge. Frames (a) and (b) show the magnetic field (in T) at $t=-250$ and 100 ps with respect to the pulse peak, respectively.

$$\frac{\partial \vec{B}}{\partial t} = \vec{\nabla} \times \left(\frac{c}{en_e} \vec{\nabla} P_e \right) + \vec{\nabla} \times [(\vec{u} + \vec{V}_n) \times \vec{B}] - \frac{c^2}{4\pi} \vec{\nabla} \times \left(\frac{\vec{\nabla} \times \vec{B}}{\sigma} \right), \quad (1)$$

where $P_e=n_e k_B T_e$ is the electron pressure, $\vec{u}$ is the average fluid velocity, $\vec{V}_n \sim -0.71\kappa\vec{\nabla}T_e/n_e T_e$ is the Nernst velocity, κ is the thermal conductivity, and σ is the Spitzer electrical conductivity. The only source term for the magnetic field is thus

$$\vec{\nabla} \times \left(\frac{c}{en_e} \vec{\nabla} P_e \right) = -\frac{k_B c}{en_e} \vec{\nabla} n_e \times \vec{\nabla} T_e. \quad (2)$$

Figure 6 shows the azimuthal magnetic field distribution at two different times. The region where the magnetic field is stronger extends over $\sim$90 μm and corresponds to densities of $\sim 5\times10^{20}$ cm^{-3}. The maximum value is $\sim$50 T, which is found $\sim$100 μm away from the expansion axis and $\sim$50 μm from the original target surface. Near the axis, the magnetic field is weaker and has an opposite sign with an amplitude of $\sim$5 T at $t=-250$ ps in a small region localized at about 10 μm from the axis and extending over 20 μm, corresponding to densities of $\sim 2\times10^{21}$ cm^{-3}. The simulations also show the presence on an electric field along the pressure gradients and with a maximum amplitude slightly lower than 1×10^8 V/m.

The CHIC simulations were also used to study the relaxation of the plasma with an initial nonaxially symmetric distribution as may be generated due to the elliptical laser spot. 2D CHIC simulations were run in the transverse x-y plane (i.e., parallel to the target plane). The initial density is uniform, equal to critical density, and the energy was deposited uniformly on an ellipse, the intensity being kept constant at 510^{14} W/cm^2. Hence, the heated volume was an infinite cylinder with the axis directed along the z-axis (perpendicular to the simulation plane) and elliptical cross section. The simulation showed that the plasma expansion becomes quasi-axisymmetric within $\sim$100 ps. This can be explained by the higher fluid velocity due to higher conductive losses at the smaller axis of the elliptical focus, which implies a quicker expansion of the system along that direction and results in a symmetrization of the global expansion. This accounts for the reasonably circular shape of the deflection patterns [e.g., Figs. 3(a) and 4].

V. PARTICLE TRACING ANALYSIS AND DISCUSSION

To confirm that azimuthal magnetic field distributions similar to those observed in CHIC simulations can produce the observed deflectometry images and to infer from the latter the values of the magnetic field amplitudes and their spatial scale, particle tracing simulations with the PTRACE code[11] have been carried out. PTRACE computes the propagation of probe protons into a given pattern of electromagnetic fields, taking the experimental geometry and the detector response into account. A suitable parametrization of the magnetic field has been inferred from CHIC simulations. The magnetic field $B_\phi=B_\phi(r,z)$ has azimuthal field lines contained in a torus with amplitude given in cylindrical coordinates (r,z,ϕ) by

$$B_\phi = B_0 F(r;r_B,L_r) G(z;z_B,L_{z1},L_{z2}), \quad (3)$$

where

$$F(r;r_B,L_r) \equiv \exp\left[-\left(\frac{r-r_B}{L_r} \right)^2 \right] - \exp\left[-\left(\frac{r+r_B}{L_r} \right)^2 \right], \quad (4)$$

$$G(z;z_B,L_{z1},L_{z2}) \equiv \exp\left[-\left(\frac{z-z_B}{L_{z1}} \right)^2 \right] \theta(z-z_B) + \exp\left[-\left(\frac{z-z_B}{L_{z2}} \right)^2 \right] \theta(z_B-z). \quad (5)$$

As inferred from the CHIC simulations, the fields evolve on times much longer than the time needed for the probe protons to cross the plasma. Thus, when attempting to reproduce a particular frame of the proton images corresponding to a given time, the temporal dependence of the fields may be ignored. The results of the particle tracing simulations are presented next to the corresponding data, see Figs. 3(b), 3(d), 4(b), 4(d), and 5(b). The values chosen for the parameters are reported in the figure captions. By tuning the parameter values, a good agreement between the experimental and PTRACE images is found both in terms of mesh pattern deflection and dose distribution. In the PTRACE simulations the contribution of an additional magnetic field component, mimicking the

field observed in the inner, dense region near the axis in the CHIC simulations [Fig. 6(a)], was also considered. However, raising the amplitude of such field up to 5 T (the peak value found in the simulation) produced no noticeable effect. In a similar way, the electric field as evaluated from CHIC simulations was found to produce just a slight deformation of the mesh lines in the central part of the deflectograms. We conclude that the observed deflections are almost entirely due to the magnetic field in the coronal region and that, since the "optimal" values for the field and scale length parameters are in fair agreement with the CHIC predictions, in this regime the main source for the magnetic field is the $\vec{\nabla}T_e \times \vec{\nabla}n_e$ term.

Shots performed at higher laser energy for the interaction beams (150 and 300 J) exhibit similar proton deflectometry patterns with the difference that in the central region of the plasma, the mesh pattern was completely deflected away (as, for example, in Ref. 13) and did not allow quantitative measurements. This can be expected since at such laser energies and intensities ($>10^{15}$ W cm^{-2}), the magnetic field in the dense plasma region can reach an amplitude greater than 100 T,[1] as also shown by the hydrodynamic simulations. For the proton energies used in this experiment ($\sim$5 MeV), the particle tracing simulations show that such fields induce complete outward deflection consistently with the experimental observation. To allow quantitative measurement of such field amplitudes, higher probing proton energies ($>$30 MeV) as can be obtained on petawatt laser facilities[17] would be needed.

VI. CONCLUSIONS

In conclusion, we measured the spatial and temporal distributions of magnetic fields resulting from the interaction between a long-pulse, high-power laser and a solid in a regime relevant for ICF physics. We have verified that the $\vec{\nabla}T_e \times \vec{\nabla}n_e$ mechanism is the dominant term producing the magnetic field in the coronal plasma at the edges of the focal spot. No significant field was detected in the inner, denser region of the plasma, implying that field amplitudes in this region are smaller than $\sim$5 T. The field amplitudes inferred from the data match well the spatial and temporal evolution of the fields as simulated by a 2D hydrodynamic code, showing that these fields can therefore be well modeled in such frame without requiring the input of alternative physical effects.

ACKNOWLEDGMENTS

We acknowledge the discussions with Dr. M. Galimberti (CLF, RAL-STFC) and the support of the RAL laser, target area, target production, and engineering teams. We also acknowledge the financial support from CCLRC, British Council/Alliance, COST funded program, EPSRC, ANDOR Technology, the IRCEP/QUB scheme, and the DFG funded programs TR18 and GK1203. A.M. acknowledges the International Research Fellowship from the Queen's University of Belfast.

[1] J. A. Stamper, Laser Part. Beams **9**, 841 (1991).
[2] J. D. Lindl, P. Amendt, R. L. Berger, S. G. Glendinning, S. H. Glenzer, S. W. Haan, R. L. Kauffman, O. L. Landen, and L. J. Suter, Phys. Plasmas **11**, 339 (2004).
[3] G. Schurtz, S. Gary, S. Hulin, C. Chenais-Popovics, J.-C. Gauthier, F. Thais, J. Breil, F. Durut, J.-L. Feugeas, P.-H. Maire, P. Nicolaï, O. Peyrusse, C. Reverdin, G. Soullié, V. Tikhonchuk, B. Villette, and C. Fourment, Phys. Rev. Lett. **98**, 095002 (2007).
[4] P. Nicolaï, M. Vandenboomgaerde, B. Canaud, and F. Chaigneau, Phys. Plasmas **7**, 4250 (2000).
[5] R. J. Mason and M. Tabak, Phys. Rev. Lett. **80**, 524 (1998).
[6] M. G. Haines, Phys. Rev. Lett. **78**, 254 (1997).
[7] O. Willi, P. T. Rumsby, and C. Duncan, Opt. Commun. **37**, 40 (1981).
[8] M. Borghesi, A. J. MacKinnon, A. R. Bell, R. Gaillard, and O. Willi, Phys. Rev. Lett. **81**, 112 (1998).
[9] A. J. Mackinnon, P. K. Patel, R. P. Town, M. J. Edwards, T. Phillips, S. C. Lerner, D. W. Price, D. Hicks, M. H. Key, S. Hatchett, S. C. Wilks, M. Borghesi, L. Romagnani, S. Kar, T. Toncian, G. Pretzler, O. Willi, M. Koenig, E. Martinolli, S. Lepape, A. Benuzzi-Mounaix, P. Audebert, J. C. Gauthier, J. King, R. Snavely, R. R. Freeman, and T. Boehly, Rev. Sci. Instrum. **75**, 3531 (2004).
[10] L. Romagnani, J. Fuchs, M. Borghesi, P. Antici, P. Audebert, F. Ceccherini, T. Cowan, T. Grismayer, S. Kar, A. Macchi, P. Mora, G. Pretzler, A. Schiavi, T. Toncian, and O. Willi, Phys. Rev. Lett. **95**, 195001 (2005).
[11] M. Borghesi, L. Romagnani, A. Schiavi, D. H. Campbell, M. G. Haines, O. Willi, A. J. Mackinnon, M. Galimberti, L. Gizzi, R. J. Clarke, and S. Hawkes, Appl. Phys. Lett. **82**, 1529 (2003).
[12] M. Borghesi, L. Romagnani, S. Kar, T. Toncian, P. Antici, P. Audebert, E. Brambrink, F. Ceccherini, C. A. Cecchetti, J. Fuchs, M. Galimberti, L. A. Gizzi, T. Grismayer, R. Jung, A. Macchi, P. Mora, J. Osterholtz, A. Schiavi, and O. Willi, in *Superstrong Fields in Plasmas: Third International Conference of Superstrong Fields in Plasma*, edited by D. Batani and M. Lontano (American Institute of Physics, Melville, 2006), p. 191.
[13] P. M. Nilson, L. Willingale, M. C. Kaluza, C. Camperidis, S. Minardi, M. S. Wei, P. Fernandes, M. Notley, S. Bandyopadhyay, M. Sherlock, R. J. Kingham, M. Tatarakis, Z. Najmudin, W. Rozmus, R. G. Evans, M. G. Haines, A. E. Dangor, and K. Krushelnick, Phys. Rev. Lett. **97**, 255001 (2006).
[14] C. K. Li, F. H. Séguin, J. A. Frenje, J. R. Rygg, R. D. Petrasso, R. P. J. Town, P. A. Amendt, S. P. Hatchett, O. L. Landen, A. J. Mackinnon, P. K. Patel, V. A. Smalyuk, T. C. Sangster, and J. P. Knauer, Phys. Rev. Lett. **97**, 135003 (2006); C. K. Li, F. H. Séguin, J. A. Frenje, J. R. Rygg, R. D. Petrasso, R. P. J. Town, P. A. Amendt, S. P. Hatchett, O. L. Landen, A. J. Mackinnon, P. K. Patel, M. Tabak, J. P. Knauer, T. C. Sangster, and V. A. Smalyuk, *ibid.* **99**, 015001 (2007).
[15] M. Tatarakis, I. Watts, F. N. Beg, E. L. Clark, A. E. Dangor, A. Gopal, M. G. Haines, P. A. Norreys, U. Wagner, M.-S. Wei, M. Zepf, and K. Krushelnick, Nature (London) **415**, 280 (2002).
[16] J. Breil, P.-H. Maire, P. Nicolaï, and G. Schurtz, J. Phys.: Conf. Ser. **112**, 022035 (2008).
[17] R. A. Snavely, M. H. Key, S. P. Hatchett, T. E. Cowan, M. Roth, T. W. Phillips, M. A. Stoyer, E. A. Henry, T. C. Sangster, M. S. Singh, S. C. Wilks, A. MacKinnon, A. Offenberger, D. M. Pennington, K. Yasuike, A. B. Langdon, B. F. Lasinski, J. Johnson, M. D. Perry, and E. M. Campbell, Phys. Rev. Lett. **85**, 2945 (2000).